ENCLOSURE 2

ATTACHMENT 8

"Engineering Report for Quad Cities Unit 1 Scale Model Testing," NEDO-33192, Non-Proprietary, dated April 2005

Non-Proprietary Version
NEDO-33192

GE Nuclear Energy

175 Curtner Avenue
San Jose, CA 95125

NEDO-33192
Class I
April 2005

Engineering Report for

Quad Cities Unit 1 Scale Model Testing

Principal Contributor

Daniel Sommerville

NON-PROPRIETARY NOTICE

IMPORTANT NOTICE

This is a non-proprietary version of the document NEDC-33192P, which has the proprietary information removed. Portions of the document that have been removed are indicated by an open and closed bracket as shown here [[ ]].

IMPORTANT NOTICE REGARDING CONTENTS OF THIS REPORT PLEASE READ CAREFULLY

The information contained in this document is furnished for the purpose of obtaining NRC approval of the licensing requirements to expand the power/flow operating range to allow operation with the licensed thermal power up to 120% of original thermal power. The only undertakings of General Electric Company with respect to information in this document are contained in contracts between General Electric Company and participating utilities, and nothing contained in this document shall be construed as changing those contracts. The use of this information by anyone other than that for which it is intended is not authorized; and with respect to **any unauthorized use**, General Electric Company makes no representation or warranty, and assumes no liability as to the completeness, accuracy, or usefulness of the information contained in this document.

ACKNOWLEDGEMENTS

The QC scale model test program was a first of a kind effort which involved a substantial amount of discovery and effort. The team assembled to solve this problem was truly multi-disciplinary. Without the assistance and support of the entire team this effort could not have been a success. I wish to thank and acknowledge the following people for their substantial contribution to this effort.

Technical Guidance and Review:	Dr. Robert Blevins, Consultant Mr. John Lynch, GE Energy Dr. Fred Moody, Consultant Mr. Daniel Pappone, GE Energy
Acoustic Modeling:	Dr. Eike Brechlin, LMS Mr. David Galbally, GE Energy Mr. Mathieu Jonckheere, LMS
Testing and Data Analysis:	Mr. Quentin Guzek, LMS Mr. Michael Nieheisel, LMS Mr. Matthew O'Connor, GE Energy
CFD Analysis:	Dr. Robert Malone, GE Energy
Test Setup & Support:	Mr. Steve DelGrande, GE Energy Mr. Henry Domec, GE Energy Mr. Teddy McDowel, GE Energy Mr. Richard Turnwall, GE Energy Mr. Dwight Springer, GE Energy Mr. Steve Wilson, GE Energy
Mechanical Design & Drafting:	Mr. Tom Lewis, GE Energy Mr. Paul Ng, GE Energy Mr. Jonathon Quach, GE Energy Mr. Jeff Sanders, GE Energy Mr. Ralph Walker, GE Energy
Project Management:	Mr. Alton Jenkins, GE Energy Mr. Edward Skeehan, GE Energy

Table of Contents

List of Tables

List of Figures

Nomenclature

ABWR	Advanced Boiling Water Reactor
AC	Alternating Current
BWR	Boiling Water Reactor
CFD	Computational Fluid Dynamics
CFM	Cubic Feet per Minute
DC	Direct Current
EPU	Extended Power Uprate
ERV	Electromatic Relief Valve
FEM	Finite Element Model
FIV	Flow Induced Vibration
FRF	Frequency Response Function
FSI	Fluid-Structure Interaction
GE	General Electric Company
GENE	General Electric Nuclear Energy
HPCI	High Pressure Core Injection
ID	Inner Diameter
IGSCC	Inter Grannular Stress Corrosion Cracking
IVVI	In Vessel Visual Examination
LMS	Lueven Measurement Systems
MDOF	Multiple Degree of Freedom System

Nomenclature, contd.

MS	Main Steam
MSIV	Main Steam Isolation Valves
MSL	Main Steam Line
OLTP	Original Licensed Thermal Power
PC	Personal Computer
PSD	Power Spectral Density
QC	Quad Cities
QC1	Quad Cities Unit 1
QC2	Quad Cities Unit 2
RCIC	Reactor Core Isolation Cooling
RMS	Root Mean Square
RPM	Revolutions per Minute
RPV	Reactor Pressure Vessel
SDOF	Single Degree of Freedom System
S/RV	Safety and Relief Valves
SV	Safety Valve
TCV	Turbine Control Valves
TRV	Target Rock Valve
TSV	Turbine Stop Valves

Nomenclature, contd.

VPF	Vane Passing Frequency
1-D	One Dimensional
3-D	Three Dimensional
c	Speed of sound in media
[c]	Damping matrix
d	Diameter of branch line and/or cavity width
E	Energy
f	Frequency of acoustic oscillation
F	Body force
[k]	Stiffness matrix
L	Length of resonating chamber
[m]	Mass matrix
M	Mach Number
n	Shear wave mode
P	Pressure
P'	Fluctuating Pressure
Re	Reynolds Number
Re_p	Reynolds number using main steam line ID as the characteristic dimension
Re_v	Reynolds number using reactor pressure vessel ID as the characteristic dimension

Nomenclature, contd.

St	Strouhal Number
t	Time
U	Mean fluid velocity
V	Velocity
X	Geometric scaling factor and/or displacement
X''	Acceleration
y	Displacement
y'	Velocity
y''	Acceleration
λ	Wavelength
ρ	Fluid Density
ω	Circular Frequency

Subscripts

A	Plant A
m	Model
QC	Quad Cities
p	Plant

Executive Summary

Several incidences of high cycle fatigue cracking have been observed in the steam dryers at Dresden and Quad Cities following operation at extended power uprate conditions for a relatively short period of time. The field experience exhibited at the Quad Cities and Dresden power plants suggests that the steam dryers at these power plants experience substantial loading during normal operation. GE has previously installed repairs on the original Quad Cities dryer designs; however, GE is now designing a new dryer for installation in the Quad Cities and Dresden units. To assist in creating a load definition for this new dryer and to improve the general understanding of the characteristics of the fluctuating loads acting upon the BWR steam dryers, GE has designed and built a scale model test facility. This document summarizes the conclusions made from review of currently available in-vessel data as well as the results of multiple tests performed with scale models of the QC1 plant configuration. Both the original and replacement dryer designs were tested. The scale model test data is benchmarked against the available plant data to provide an interim assessment of the validity of the scale model test method and scaling factors. The following conclusions are made from the plant data review:

1. The fluctuating pressure load spectra shown by the in-plant measurements indicate that the characteristics of the pressure loading on the steam dryer is similar for all BWRs, regardless of vessel size or steam dryer hood design.

2. Acoustic induced vibration is considered to be the dominant excitation mechanism for the steam dryer

3. Flow turbulence and vortex shedding are both considered possible excitation mechanisms for the acoustics observed in the plant data

4. It is believed that flow turbulence and shear layer instabilities are each separately responsible for exciting portions of the frequency content observed in the vessels of three separate BWRs. It is also believed that the data obtained from these three plants is representative of the type of fluctuating loads expected in Quad Cities and Dresden.

   [[

]]

The following conclusions are made from the model testing:

1. The scale model test data match well with the available in-plant data; therefore,

    a. The scale model test apparatus and methodology are viable tools to predict fluctuating pressure loads on the steam dryer.

    b. The decision that acoustic loads are the primary contribution to the fluctuating loads on the BWR steam dryer is validated.

    c. The model data appear to be conservative in the 30-100 Hz frequency band at the plant scale.

    d. Considering the startup testing and acceptance criteria planned for the QC replacement dryer, the QC model data acquired from the Baseline tests are considered an acceptable input for a QC dryer load definition.

2. The fluctuating pressures used as inputs in the scale model based QC replacement dryer load definition can be explained by the following:

3. Recognizing the similarity between the QC1 & 2 steam plenum and steam line designs, the QC1 model data is considered to be applicable to both Quad Cities Unit 1 & 2.

The scale model data will be benchmarked against the Quad Cites in-vessel data when it is available. Additional work is on-going to improve the understanding of the excitation mechanisms and source locations. The work described in this document is the beginning of a substantial amount of research focused on developing predictive tools that can be used to define accurate load definitions for BWR steam dryers.

1.0 Scope

This report provides the engineering basis for the scale model test apparatus and methodology. From this document the reader is expected to obtain an understanding of the following items:

- General characteristics of the unsteady fluid loading observed in other BWR steam systems
- Technical basis for investigating acoustic induced vibration as the dominant flow induced vibration load mechanism
- General understanding of the GE scale model test apparatus and methodology
- Scale model testing performed to date
- General characteristics of QC1 scale model test data and important observations
- Characteristics of the data used for the scale model test based load definition for the replacement QC dryer design.
- Preliminary justification of scale model test data

This document is not intended to be a detailed test report for every test performed. All scale model test data are archived at the GENE San Jose site and the test procedures are contained in the applicable design record files.

2.0 Background

This section provides background information that should enable the reader to become familiar with the following items:

- BWR Steam dryer failures
- Metallurgical analysis of initial steam dryer failure
- General BWR configuration
- General steam dryer configuration

2.1 Quad Cities Unit 2 Steam Dryer Failure - 2002

On July 11, 2002, Quad Cities Unit 2 (QC2) was shut down due to degradation of the steam dryer. QC2 had operated approximately 90 days under Extended Power Uprate (EPU) conditions. The plant was licensed up to 117% of original licensed thermal power (OLTP). At full power, this would increase steam flow to approximately 120% of previous OLTP flow. During the end of that 90-day period, QC2 experienced several anomalous readings related to reactor pressure, reactor water level, steam flow, and steam line moisture content.

Following plant shutdown, an inspection of the QC2 plant revealed that a steam dryer cover plate had failed (See Figure 1), allowing steam to bypass the dryer flow path. The root cause investigation of the QC2 cover plate failure identified a potential cause to be high cycle fatigue generated by the near coincidence of an acoustic natural frequency in the steam plenum, the vortex shedding frequency associated with flow over the steam dryer, and the mechanical natural frequency of the cover plate. The shear layer instability was thought to be a result of steam flow past sharp discontinuities in dryer geometry (See Figures 4 through 7). At the increased steam flow rates associated with EPU the acoustic standing wave frequency and the vortex shedding frequency may have become nearly aligned which may have excited an acoustic mode in the steam plenum, causing near

resonant response at approximately 180-Hertz. This frequency is postulated to be nearly coincident with the structural natural frequency of the cover plate that failed.

Subsequent to the failure observed in 2002, additional failures were observed during 2003 in the dryer outer hoods of both Quad Cities Units 1 and 2. These failures were associated with high cycle fatigue caused by a low frequency fluctuating pressure load. Figures 1 through 3 are photographs of some of the observed failures. The steam dryers at Dresden Units 2 and 3 also showed incipient cracking at the same initiation sites as the hood cracking observed in the Quad Cities dryers, though the cracks at the Dresden units did not grow to failure.

In response to these failures GE has initiated a development program to investigate the nature of the steam dryer loading. This effort includes both model testing as well as development of acoustic and computational fluid dynamics models.

2.2 Analysis of initial steam dryer failure

Metallurgical evaluations of the fracture surfaces of the 2003 Quad Cities Unit 2 failure were performed to obtain additional information regarding the failure mechanism. The results of this evaluation support the following conclusions and observations:

1. The failure was a result of high cycle fatigue
2. Intergrannular Stress Corrosion Cracking (IGSCC) was not evident
3. No chemistry, material, or manufacturing deficiencies were observed
4. The observed cracks initiated at the local stress concentration adjacent to a stiffening bracket attachment weld beneath the horizontal cover plate

2.3 General BWR and Steam Dryer Configuration

Figures 4 and 5 describe the general BWR nuclear boiler arrangement. The steam dryer, shown to the right of the reactor pressure vessel in Figure 4, is located in the top of the vessel. Steam is generated in the reactor core then passes through the steam separators and steam dryer prior to leaving the vessel through the main steam nozzles. The general flow path of the reactor coolant is shown is Figure 5. The black arrows in this figure identify the water flow path and the white arrows depict the steam flow path. Figure 6 is a section view of the steam dryer from which the orientation of the internal dryer banks can be seen. The chevron flow paths through the dryer vane banks remove moisture from the steam.

Liquid is removed from the steam as the flow passes through the steam separators and steam dryer; the steam leaves the dryer with a quality of approximately 99.9%. The steam exits the reactor pressure vessel through each of four separate main steam nozzles. The orientation of the main steam nozzles with respect to the steam dryer is shown in Figure 7. This figure illustrates one side of the steam dryer; as can be seen in the previous figures, the steam dryer is symmetric and the other two main steam nozzles are diametrically opposed to those shown in Figure 7. Once the steam leaves the reactor pressure vessel it is routed to the turbine through the main steam piping. The piping contains multiple elbows and flow restrictions such as: venturis, Main Steam Isolation Valves (MSIV), equalizing headers, and Turbine Control and Stop Valves (TCV, TSV). Figures 8 and 9 are schematics of a typical main steam line routing from the RPV to the turbine. Main steam line systems also have smaller diameter branch lines connected to the main steam lines such as Safety and Relief Valve (S/RV) standpipes and extraction lines for HPCI, RCIC and feedwater pump turbines. These branch lines are not shown in Figures 8 and 9. The specific dimensions of the steam piping vary according to the plant power output and balance of plant layout. The nominal main steam line piping ranges between 16 and 28 inches in diameter.

The steam in the main steam lines and steam plenum of a BWR can generally be described by the following parameters:

Pressure:	1000-1050 psig
Temperature:	540 °F
Density:	2.24 lb/ft^3
Dynamic Viscosity:	0.0459 lb/(hr-ft)
Quality:	> 99 %
Sound Speed:	1600 ft/s
Steam Velocity in MSL:	120 ft/s – 200 ft/s

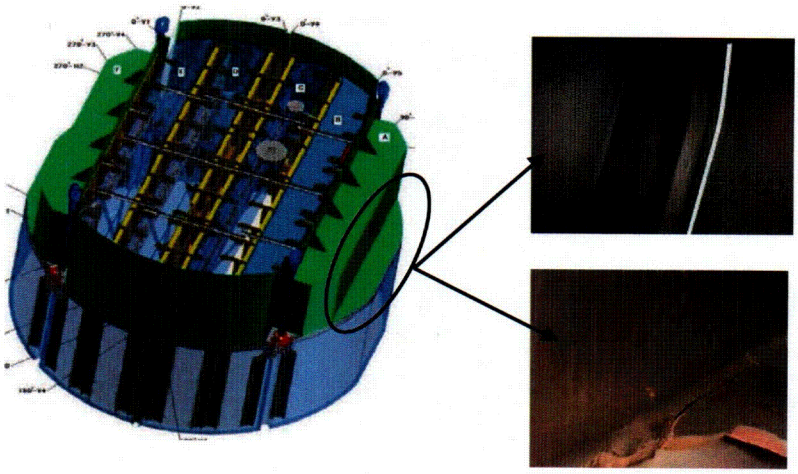

Figure 1: Photograph of cover plate failure

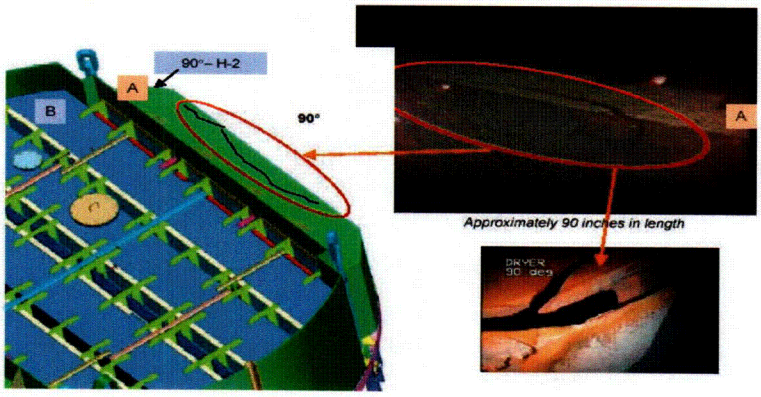

Figure 2: Photograph of vertical hood failure

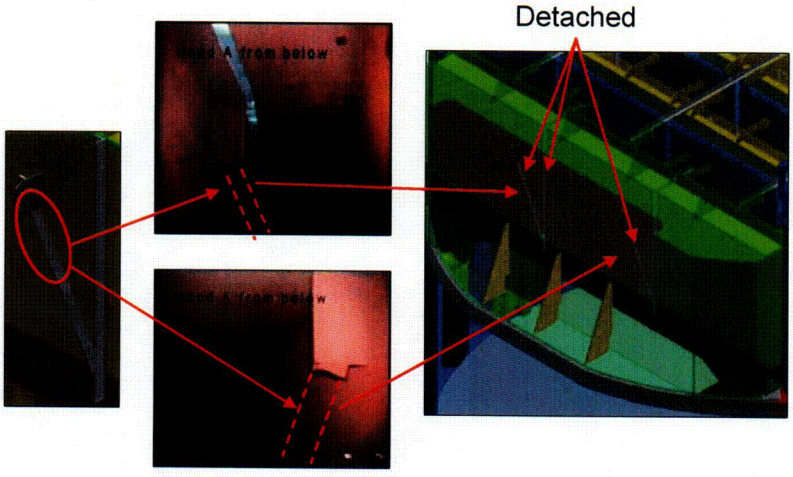

Figure 3: Photograph of diagonal brace failure

C01

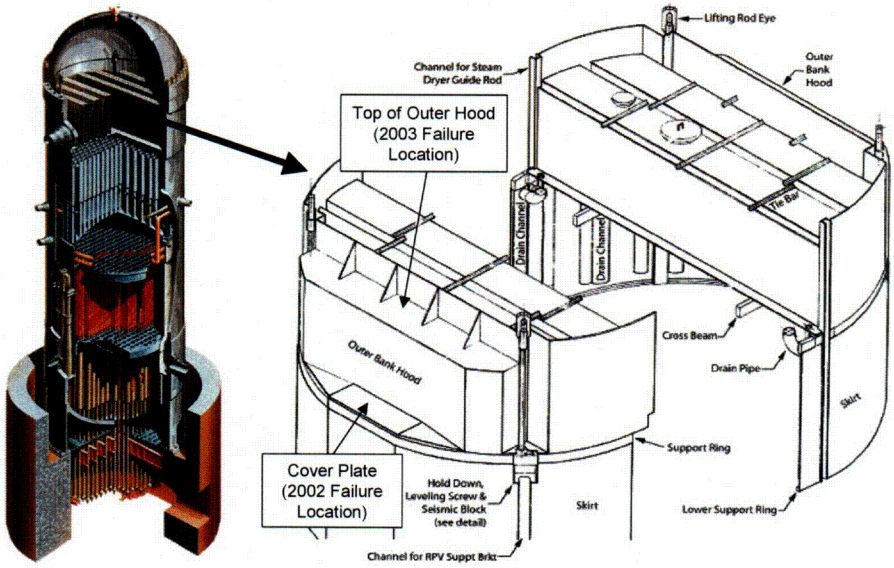

Figure 4: General schematic of the RPV and steam dryer

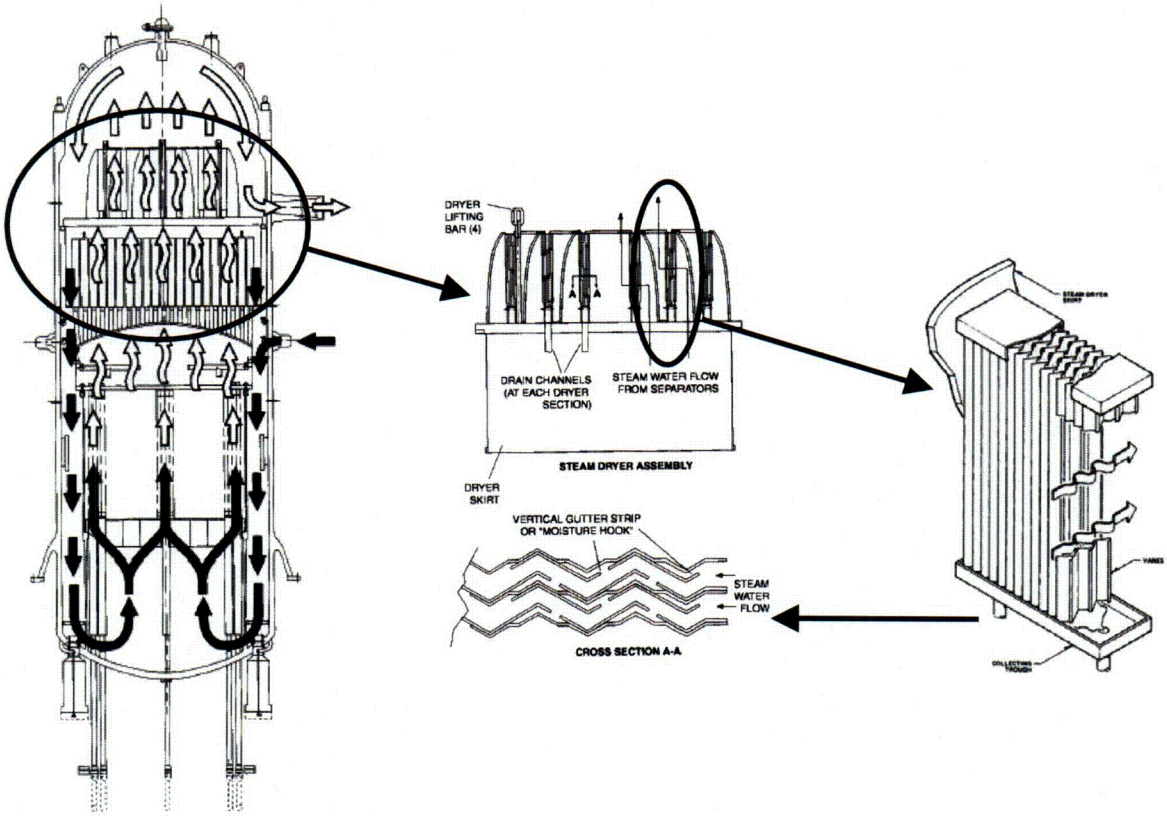

Figure 5: Coolant flow path through reactor pressure vessel

C02

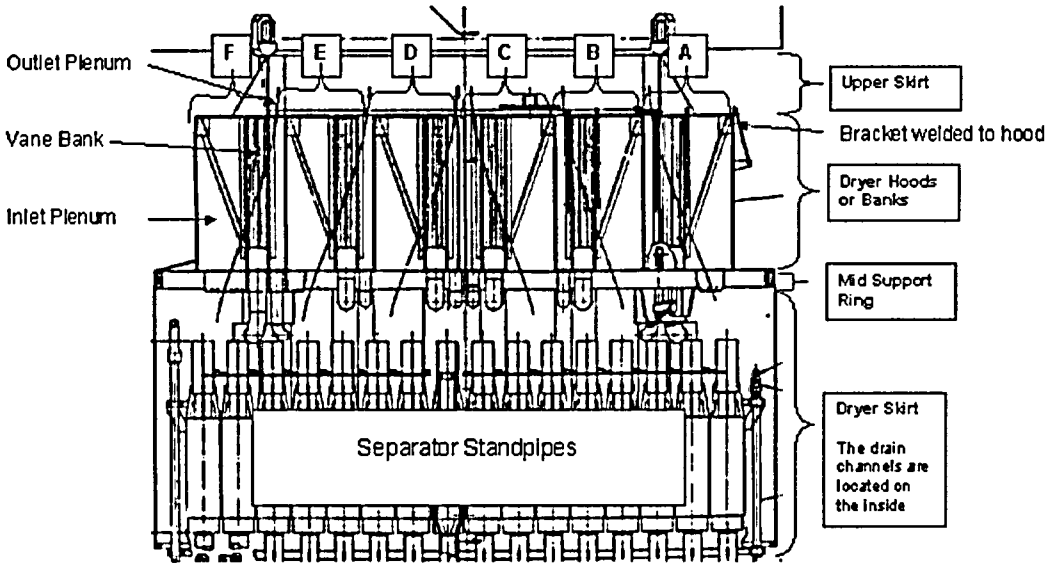

Figure 6: Section view of a BWR steam dryer and steam separator

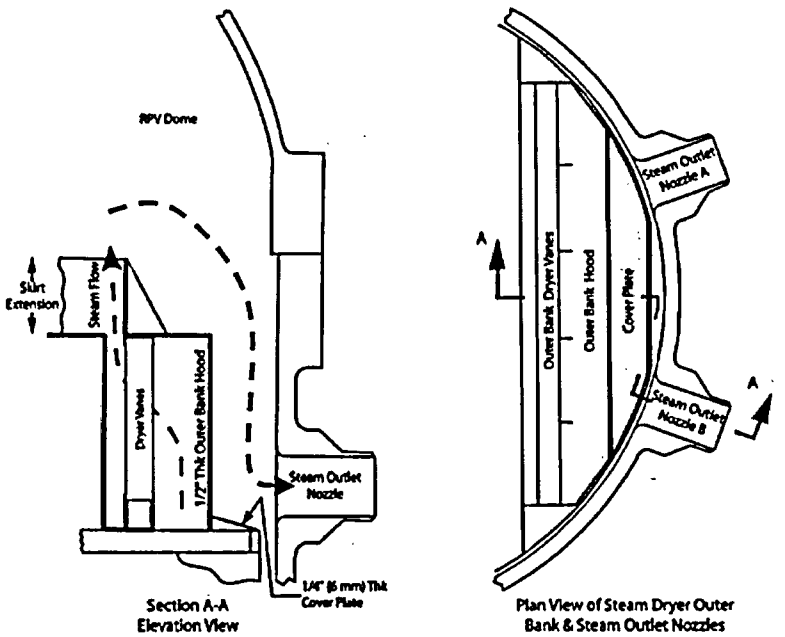

Figure 7: Orientation of main steam nozzles to steam dryer

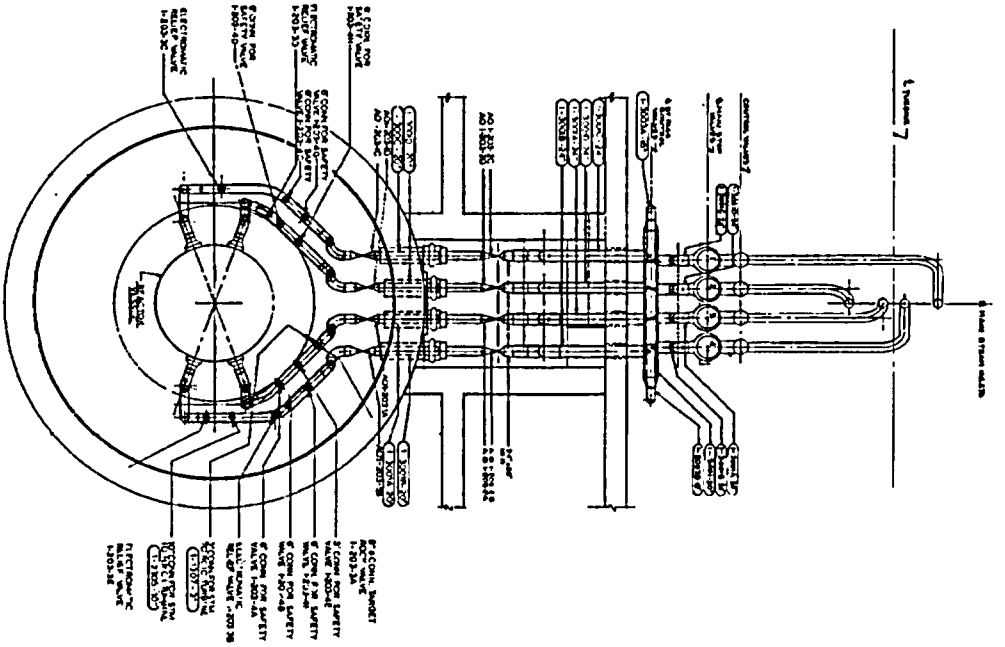

Figure 8: Plan view of a main steam line layout between RPV and turbine

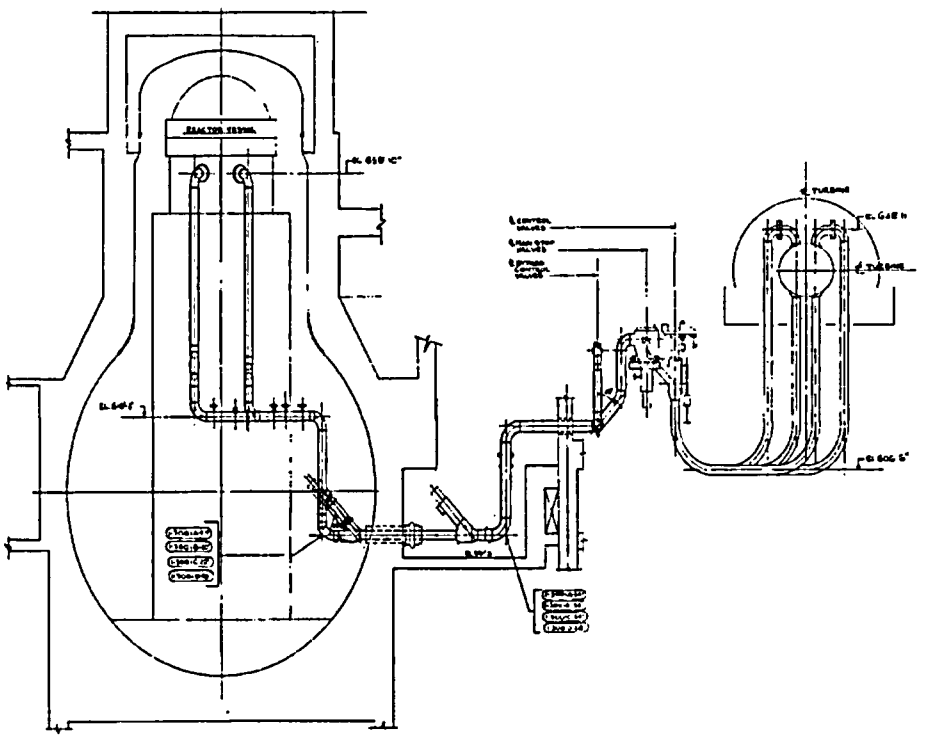

Figure 9: Elevation view of a main steam line layout between RPV and turbine

3.0 Fluctuating Pressure Loads on BWR Steam Dryers

This section summarizes and analyzes the existing data available from in-vessel steam dryer instrumentation programs performed during reactor startup power ascension test programs and dryer repair test programs. The results of the data characterizations are compared to identified theoretical and technical literature to characterize the important processes involved in dryer loading and vibration response. This data has been used for benchmarking of the GE scale model test program. Further benchmarking and test validation will be performed when additional in-plant data is available from the new Quad Cities dryer startup program. The frequencies discussed in this section are reported at the plant scale; in Section 6 model data is presented in which the frequencies are in the model scale. The model data must be corrected to the plant scale using the frequency scaling factor provided in Section 5.2.2 to be compared to the data presented in this section.

3.1 Sample Population

Although the steam dryer degradation from Quad Cities described above is the most significant in-service damage observed in BWR steam dryers, it is not the first recorded example of steam dryer cracking. Various instances of cracking in tie bars, skirts, and hoods have been observed in reactors operating at original licensed power. This cracking has been attributed to either high cycle fatigue or IGSCC. Typically this cracking has been minor and could be addressed by stop drilling the crack or by repairing the cracked components. Although the source of the loading causing the fatigue cracks was never identified, successful repairs were installed and the components were returned to service without exhibiting any future problems. In a few cases, in-vessel instrumentation programs were conducted. The purpose of these instrumentation programs was to demonstrate adequacy of the repair rather than identify the nature of the loading; therefore, the instrumentation used typically consisted of strain gauges and accelerometers.

Pressure transducers have been installed on the steam dryers of only three of the approximately 60 operating BWRs in the commercial fleet. The data from each of these units have been reviewed for this survey. The data were obtained from a BWR/3, BWR/4, and an ABWR. These three plant types have substantially different RPV and MSL diameters; however, their overall geometry is similar. The BWR/3 has a square hood dryer; the BWR/4 and ABWR both have curved hood dryers.

From this sample population, data was available from 20 pressure transducers. Of these there exist 8 pairs (16 total) located on both the inside and outside of the steam dryer skirt, 2 in the steam plenum above the steam dryer, and 2 on the cover plates adjacent to the main steam nozzles. The two gauges placed on the steam dryer cover plates were strain gauges mounted on a pressure drum; therefore, the applied pressure is determined from the strain induced in the drum.

Power ascension data is available from two of the three plants. These data were obtained from 20-100% and 50-100% power. Data is currently available from the third plant at 100% power only. Table 1 summarizes the vessel diameter, average steam line velocity, approximate Reynolds number based on MSL ID, plant vintage, and steam dryer hood design for each plant from which data is available.

Table 1: Summary of sample population

Plant	RPV Diameter, in (mm)	Average MSL velocity, ft/s (m/s)	Reynolds Number, Re_D	Vintage	Dryer Hood Design
A	188 (4775)	149 (45.4)	3.1E7	BWR/3	Square
B	251 (6375)	129 (39.3)	4.6E7	BWR/4	Curved
C	280 (7112)	139 (42.4)	5.1E7	ABWR	Curved

3.2 Data Analysis

The following items are presented in this section:

- Data Analysis Methods
- Fluid Loads
  - Frequency content vs. flow
  - Amplitude vs. flow
  - Peak hold spectra
- Structural Response
  - Strain gauge data

Although the primary focus of this section is the fluctuating loads observed in the BWR steam plenum, both the fluctuating pressure loads measured by the pressure transducers as well as the dynamic strain measured by the strain gauges mounted on the steam dryers are presented here. The latter is included to provide information regarding the bandwidth of the loading that should be considered to obtain a reliable steam dryer durability assessment.

3.2.1 Data Analysis Methods

Plant data was analyzed with both an HP3566 dynamic signal analyzer and a LMS SCADAS III dynamic signal analyzer. The sampling rate was determined using the Nyquist theorem to obtain accurate frequency content in excess of 300 Hz. Peak hold spectra as well as linear averaged RMS spectra were typically used to investigate the data. All data were digitized from the original analog media used to record and store the data during the original plant testing.

The individual spectra created from the data available at each power level were combined to form color maps and waterfalls to visualize trends in the pressure and strain data as the reactor power level increased. Frequency bands or sections were selected and cut from these plots to obtain RMS levels of specific frequency bands versus power level. These frequency bands were then compared to similar information from other plants and also curve-fit to observe characteristics of the data.

3.2.2 Fluid Loads

Figures 10 and 11 are color maps exhibiting the trend of fluctuating pressure amplitude with reactor power level. The horizontal axis displays frequency, the vertical axis corresponds to reactor power level and the color scale depicts pressure amplitude. Power ascension data is available for Plants A and C only. Figures 12 and 13 express the data shown in Figures 10 and 11 as frequency spectra from each power level overlaid on the same plot. These plots are provided for convenience; color maps are convenient to visualize trends in frequency with flow; however, it is not easy to identify the specific frequency of peaks on a color map. For these two plants it is apparent that the frequency spectra can be separated into two regions exhibiting different behaviors:

- $f < 100$ Hz
- $f > 100$ Hz.

Focusing first on the frequency band between 0-100 Hz it is evident that there are multiple prominent frequency peaks observable in the data. For each of these peaks, the amplitude increases as the reactor power level is increased; however, the frequency remains constant. Steam flow is approximately proportional to reactor power level. To better understand the trend of fluctuating pressure amplitude with flow rate at each frequency, the pressure amplitudes for frequency bands centered around some of the frequencies observable in Figures 10 through 13 are displayed in Figure 14. Also shown are power law curve fit equations for the fluctuating pressure trends. These trends are

typical of the data obtained from Plants A and C. It is apparent that the pressure oscillations can be approximated by the following relationship:

$$P = A \cdot U^b \qquad (1)$$

Where: P is the fluctuating pressure amplitude
A is a reference pressure
U is the mean fluid velocity
b is the power law exponent,
[[

]] Considering this no attempt has been made to curve fit the data in this frequency range.

Figure 15 displays the frequency spectra obtained from two sensors located on both sides of the dryer skirt at Plant A. [[

]]

Also shown in this figure is the frequency spectrum of the difference between the inside and outside pressure measurements (P1-P2). [[

]] The trends shown in this plot are generally representative of those shown by the other sensor pairs at Plant A.

3.2.3 Structural Response

Figure 16 is a color map of the frequency content of power ascension data obtained from a strain gauge mounted on the outer hood of the dryer at Plant A. [[

]] Figures 17 and 18 are overlaid frequency spectra of the data obtained from strain gauges mounted on the inner hood at Plant C and the outer hood at Plant A. [[

]]

3.3 Evaluation of Plant Data

Unsteady CFD analyses of the plant configurations for which data are available have not been performed at this time. Considering the size and complexity of these systems it is doubtful that this type of analysis will be undertaken for the BWR steam system; therefore, simpler means are used here to infer possible source mechanisms and to develop possible explanations for the frequencies observed in the data evaluated for this work. The process of evaluating possible explanations for the observed plant behavior will consist of:

1) Discussion of Flow Induced Vibration (FIV) mechanisms

2) Evaluation of each FIV mechanism considering the plant vessel and piping configuration

3.3.1 Flow Induced Vibration Mechanisms

Examples of structural vibration induced by fluid flow are found in many industries. The existence of this class of problem is so common that a unique term has been coined to describe it, Flow Induced Vibration. FIV has been the subject of substantial research for many decades; from this effort various FIV mechanisms have been identified and classified as separate phenomena. Au-Yang [1] and Blevins [2] have written informative monographs that provide a thorough introduction to the common types of flow induced vibration experienced in industrial systems. The following are the most common FIV mechanisms:

- Galloping/Flutter
- Fluid-Elastic Instability
- Turbulence Induced Vibration
- Vortex Induced Vibration
- Acoustic Vibration

3.3.1.1 Galloping/Flutter and other Fluid-Elastic Instabilities

From Reference 2 it is evident that Galloping and Flutter are typically are of concern for lightweight flexible structures in which the span-wise dimension is much greater than the in-plane dimensions. Chimneys, airfoils, heat exchanger tubes and power lines are excellent examples of the types of structures for which these mechanisms should be a concern. Alternately internal or external axial flow can also cause fluid-elastic instabilities of thin walled piping. Here, again, the critical characteristic of the mechanical system is that it is long and flexible. [[

]]

3.3.1.2 Turbulence Induced Vibration

Turbulence induced vibration can be an excitation mechanism affecting structural components; however, review of discussion and sample data contained in both Au-Yang [1] and Blevins [2] show the frequency content created by turbulent loading on a structure tends to exhibit [[

]]

3.3.1.3 Vortex Induced Vibration

Vortex shedding is also known to excite structures. Typically this is a problem for long slender structures subjected to cross-flow. As vortices are alternately shed from opposite sides of the structure an oscillating force is imposed on the structure normal to the flow direction. [[

]]

3.3.1.4 Acoustic Induced Vibration

Power and process plant piping systems have long been known to be susceptible to acoustic resonance during operation. Pipe runs, cavities formed by valve bodies, closed end branch lines, and pressure vessels form resonating chambers that can be excited by a variety of excitation mechanisms. Acoustic resonances are typically observed as high amplitude narrow frequency peaks. The plant data shown in Figures 10 through 13 exhibit this characteristic which suggests that acoustic induced vibration is the primary load mechanism that should be considered. It is known that fluctuating pressure oscillations in fluid systems can be caused by the following factors:

- Mechanical
  - Periodic valve motion
  - Pump, compressor operation
- Internal Flow
  - Flow through an orifice or other abrupt geometric discontinuity
  - Flow through elbows
- External Flow
  - Turbulent flow
  - Vortex Shedding from flow across bluff bodies

Periodic valve motion can cause pressure pulses in a fluid system which can excite structural response or fluid acoustic modes. This valve motion may be the result of feedback from the fluid system or control logic that causes the valve position to oscillate about a set point.

Pumps and compressors are also known to introduce periodic acoustic pressure pulses to the working fluid. The frequencies expected from these components can be determined by considering the speed of the device (RPM) and the number of vanes on the rotor. The fundamental vane passing frequency as well as its higher harmonics can be transmitted to the fluid.

In some cases flow through valves has been shown to excite local valve body acoustic modes, standing waves in upstream or downstream piping, and emit broadband noise that can cause fatigue damage to adjacent piping [3,4]. Elbows have also been shown to cause turbulent flow that can emit broadband noise [5]. These studies also suggest that currently, the only way to reliably predict the existence of valve noise is through model testing programs.

Bluff bodies exposed to external flow will shed vortices with a certain periodicity [1, 2]. This periodic vortex shedding has been observed to excite acoustic resonances in ducts. In a similar manner shear layer instabilities have also been shown to excite acoustic oscillations in closed side branches [6].

There are many examples in the literature of aero-acoustic excitation of piping systems and the resultant degradation of components in these systems. Vibration caused by acoustic resonance in the standpipes of safety and relief valves has been a common problem in piping systems. Baldwin and Simmons [7] summarize operational experiences in which S/RV resonances were observed and provide guidelines that can be used to predict susceptibility of an S/RV to an aero-acoustic resonance. They also recommend potential mitigation techniques for problem valves. S/RV acoustic resonances can be grouped into a broader category in which a self-sustained acoustic

oscillation is induced in a cavity by flow across the cavity mouth. Rockwell and Naudascher [8] have prepared an excellent review of literature related to this phenomenon. Although there are a large number of articles regarding piping acoustics in the literature, there appears to be little discussion regarding sonic fatigue of components inside large pressure vessels.

Although the focus of this section is the evaluation of available plant data the results of some CFD analyses of the steam dryer will be briefly discussed considering their relevance to the topic considered here. [[

]]

The following sections evaluate the typical BWR plant piping and vessel configuration with respect to their potential to exhibit the various acoustic excitation mechanisms discussed above.

3.3.2 Plant Piping Configuration

[[

]] During normal operation all valves in the main steam system either have constant position or can be considered quasi-static for the time scale considered here; therefore, excitation of steam system acoustics by valve motion is not considered to be a possibility.

Other than the high pressure turbine and feedwater pump turbines, there are no pumps, compressors or other mechanical equipment that interact with the flow in the main steam piping system. Although it is possible that the vane passing frequencies from the turbines could introduce pressure oscillations in the main steam system, the normal operating speeds of the turbines and the number of vanes on the turbine shafts would create acoustic frequencies higher than observed in the data presented here. [[

]]

A review of the fluid flow path in the BWR steam system (Figures 8 and 9) shows that the steam passes through multiple elbows. Elbows are known sources of broadband turbulent noise; therefore, piping acoustics excited by this noise should be considered.

Also shown in Figures 8 and 9, is the presence of multiple valves in the main steam lines. No model testing of any of the typical BWR steam line valves has been performed; therefore, it can only be said that the MSIVs, TSVs, and TCVs, may produce noise that can excite the steam line acoustic modes. It is believed that model testing is the only practical method to examine if the various MSL valves contribute to the sound observed in the RPV. The valves must be considered a possible excitation mechanism.

[[

]]

$$f = \frac{c}{2 \cdot L} = \frac{1600 \cdot ft/s}{2 \cdot 200 \cdot ft} = 4 \cdot Hz$$

[[

]]

$$f = \frac{c}{\left[4(L + 0.6\frac{d}{2})\right]} \qquad (3)$$

[[

		]]

Sound induced by flow over cavities has been observed to occur at specific shear wave modes [2]. Reference 2 presents the following correlation to predict the vortex shedding frequency as a function of shear wave mode, n, free stream velocity, U, and cavity width, d:

$$f_n = 0.33(n - \frac{1}{4})\frac{U}{d} \qquad (4)$$

Equation (4) can be manipulated to yield the Strouhal numbers associated with each shear wave mode. It should be noted that there is substantial scatter in the St data presented for cavity resonances. Blevins [2] reports deep cavity resonance data in which the St varies between 0.25 and 1.25 and Baldwin & Simmons [7] report data in which the St ranges between 0.3 and 0.6. Recognizing that the flow rate at which resonance is created is affected by the entrance radius as well as upstream and downstream piping it is conceivable that the scatter observable in the available data is partially a result of these factors. Considering the sensitivity to these parameters the St numbers presented in Table 3 should only be considered as general values around which a deep cavity resonance may be expected to occur.

Table 3: Strouhal numbers associated with first two shear wave modes for deep cavities.

Mode	Strouhal Number
1	0.25
2	0.58

Table 4 summarizes the St numbers calculated for the frequencies greater than 100 Hz observed in the Plant A and Plant C data. The St numbers reported here were determined at the flow rate where the peak amplitude was observed. [[

]] This trend is consistent with discussions in the literature regarding aero-acoustic resonances in cavities [10].

Table 4: Summary of St number for approximate peak resonances observed in data.

]]

Summarizing the above discussion:

[[

]]

3.3.3 Vessel Configuration

Similar to the discussion provided for the main steam lines, each of the excitation mechanisms introduced above will be evaluated here with respect to the RPV configuration.

The reactor pressure vessel can experience transient loads emanating from the main steam lines when a MSIV or a S/RV is closed/opened; however, these are off-normal conditions. The fatigue cracking observed in the steam dryers occurred during normal operation. There are no other valves connected to the RPV steam plenum which cycle during normal operation; [[

]]

The large pumps connected to the RPV are the recirculation pumps and the feedwater pumps. There have been examples of resonances in BWR internals being excited by recirculation pump Vane Passing Frequencies (VPF); however, these incidents have occurred in components that are either in the recirculation system or in the submerged portion of the vessel. [[

]]

The steam flow path begins in the reactor core as water is boiled as it passes through the fuel bundles. This steam flows through a set of steam separators and dryer vanes. The steam quality at the outlet of the steam separators is ~90% and the flow velocity is low. [[

]]

After the steam exits upward from the steam dryer it enters the steam plenum in the reactor top head. The steam is redirected by the top head and flows downward into a smaller cavity between the RPV and steam dryer before it exits the vessel through the MSL nozzles as shown in Figure 5, and 22 through 24. As the flow enters the smaller cavity close to the MSL nozzles it impinges on the top plate of the steam dryer. This flow configuration is similar to flow over a step and/or a shallow cavity. Equation (4) can be used to estimate the vortex shedding frequency for turbulent flow over a step [2]. [[

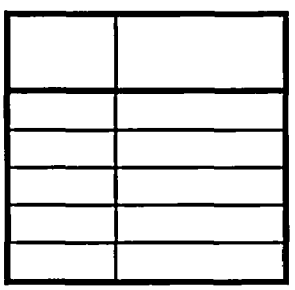

]]

The values assumed for U and d are reasonable considering a typical dryer geometry and the expected steam velocities in the steam plenum as the flow passes across the top plate of the dryer. Shallow cavity data suggest that multiple shear wave modes can exist simultaneously [8]. It should be recognized that these values are approximate and are intended only to illustrate the general range of expected vortex shedding frequencies in this region. The actual frequencies can be expected to vary about these numbers depending on specific dryer geometries, MSL diameters, and reactor power level. [[

]] A detailed acoustic finite element analysis of Plants A, B, and C has not been performed; however, the RPV cavity modes are approximated by correcting the normal modes calculated for the QC1 scale model to plant conditions using the frequency scaling relationships derived for the GE scale testing methodology (See Section 4.1) then scaling the normal modes by the RPV diameters for plant A, B, and C. Table 6 presents the estimated RPV acoustic cavity modes for plants A, B, C. It must be noted that the steam dryer designs at these three plants are different than the steam dryer used in the QC1 scale model. Recognizing this difference the values presented in Table 6 are only approximate and are intended to "roughly" approximate the expected natural frequencies of the steam plenum at these plants. The lowest modes of the vessel will be controlled by the large scale vessel geometry rather than local features on the various steam dryer designs. The RPV shape for every BWR is similar.

[[

]]

3.3.4 Summary of FIV Discussion

The significant points from the Flow Induced Vibration discussion are summarized below:

1. The fluctuating pressure load spectra shown by the in-plant measurements indicate that the characteristics of the pressure loading on the steam dryer is similar for all BWRs, regardless of vessel size or steam dryer hood design.

2. Acoustic induced vibration is considered to be the dominant excitation mechanism for the steam dryer

3. Flow turbulence and vortex shedding are both considered possible excitation mechanisms for the acoustics observed in the plant data

[[

]]

3.4 Discussion of Possibility of Fluid-Structure Interaction

Fluid Structure Interaction (FSI) is a broad term used to describe a variety of mechanisms through which the dynamics of a structure couples to the dynamics of a fluid medium. A fluid/structure problem can be described as either "strongly" or "weakly" coupled where the adjective denotes the relative importance of FSI in determining the behavior of the system. In a rigorous evaluation the equations of fluid motion would be solved with the equations of structural motion [1].

Equations of Fluid Dynamics:

Continuity:
$$\frac{\partial \rho}{\partial t} + \nabla(\rho \vec{V}) = 0 \quad (5)$$

Momentum:
$$\frac{\partial \vec{V}}{\partial t} + \vec{V} \bullet \nabla \vec{V} + \frac{\nabla P}{\rho} - \vec{F} = 0 \quad (6)$$

Energy:
$$\frac{\partial E}{\partial t} + \nabla \bullet (E\vec{V} + P\vec{V}) - \rho \vec{F} \bullet \vec{V} = 0 \quad (7)$$

Where

$$E = \rho e + \rho \vec{V} \bullet \vec{V} / 2$$

Equations of Structural Dynamics:

$$[m]\{y''\} + [c]\{y'\} + [k]\{y\} = \{F\} \quad (8)$$

The equation of structural motion is expressed in matrix notation above. The fluid equations are expressed in vector notation. These two systems are coupled by the requirement that the fluid velocity normal to the structure be equivalent to the normal component of the structural velocity at the surface. It is apparent that these equations do not lend themselves to a simple solution and it is because of this fact that system models are simplified for analysis when possible.

The interaction or coupling between the fluid and the structure can be observed in the following ways:

- Structural deflection changes the flow pattern
- Structural deflection changes the characteristic acoustic modes of the cavity
- Immersion of the structure in fluid affects the dynamic characteristics of the structure.
- Structural motion while immersed in fluid introduces an energy loss mechanism through which energy is radiated into the fluid.

3.4.1 Fluid Structure Coupling Resulting from Large Structural Displacements

The first two concepts introduced above require very large structural displacements to occur before the fluid flow patterns are substantially disturbed or the acoustic cavity created by the steam plenum is changed enough to affect the lower modes of interest (0-200 Hz). Obviously the response of each steam dryer will depend not only on the steam dryer structural design but also on the fluid loading applied to it; therefore, no single evaluation can be said to bound all configurations. Even so, it can be said that the BWR steam plenum configuration and the various steam dryer structures are not so dissimilar that the behavior of any one system will be expected to be drastically different than another. Considering the RPV and steam dryer geometry it can be expected that the dryer panels would have to experience displacements on the order of 6-12 inches before the fluid path would either be substantially disturbed or the natural frequencies of the cavity would begin to change.

Available plant data from instrumented dryers has been reviewed to determine the amplitude of displacements observed at three different plants. From accelerometer measurements the structural displacement can be determined by integrating the acceleration signal twice. Assuming a harmonic acceleration the structural displacement can also be determined by dividing the amplitude of the acceleration by the square of the frequency of oscillation in rad/s:

$$X = \frac{X''}{\omega^2} \qquad (9)$$

Consistent with the plant data observations described above, two frequency bands are considered here:[[ ]]. The maximum acceleration observed in all of the available data from Plant A in these frequency ranges is used with the lowest observed frequency peak to estimate a bounding structural displacement.

[[

]]

$$X_2 = \frac{2(32.2\frac{ft}{s^2})}{[2\pi(180Hz)]^2} = 0.0006in$$

[[

]]

3.4.2 Hydrodynamic Mass and Acoustic Radiation Damping

Immersion of a structure in a fluid with a density similar to that of the structure can introduce additional phenomena which should be considered to obtain an accurate prediction of the structural behavior. Hydrodynamic mass and Radiation damping pertain only to the response of the structure and do not affect the fluid behavior; therefore, it is not necessary to consider them for the model testing program. The scale model is

intended only to model the fluid behavior in the steam plenum; the model is not intended to be dynamically similar to the plant structure.

3.4.3 Structural Resonance

An additional condition which must be considered is the effect of a simultaneous existence of a forcing function with a structural mode. This coincidence of forcing mode shape and frequency with structural mode shape and frequency is best described as the structure being driven at or near resonance. Because the response of the structure at resonance is not sufficient in and of itself to affect the fluid load acting on the structure, this is not, strictly speaking, FSI; however, it is an important consideration when the mechanical system contains structural modes with more than one degree of freedom. For a SDOF system it is only necessary to consider the excitation frequency when determining if resonance is a concern. For a MDOF system it becomes important to consider both the frequency and distribution of the load and the system response. The model test program is designed to acquire data that describes both the frequency content and spatial distribution of the fluid loading. In addition, the structural evaluation considers the dynamic response of the structure; therefore, the methods applied for this evaluation are adequate to address structural resonance.

3.5 Conclusions

The data presented herein suggest the following conclusions:

1. The fluctuating pressure load spectra shown by the in-plant measurements indicate that the characteristics of the pressure loading on the steam dryer is similar for all BWRs, regardless of vessel size or steam dryer hood design.

2. Acoustic induced vibration is considered to be the dominant excitation mechanism for the steam dryer

3. Flow turbulence and vortex shedding are both considered possible excitation mechanisms for the acoustics observed in the plant data

4. It is believed that flow turbulence and shear layer instabilities are each separately responsible for exciting portions of the frequency content observed in the vessels of three separate BWRs. It is also believed that the data obtained from these three plants is representative of the type of fluctuating loads expected in Quad Cities and Dresden.

[[

]]

[[

]]

Figure 10: 0-Peak power ascension colormap of pressure transducer from Plant A.

[[

]]

Figure 11: 0-Peak power ascension colormap of pressure transducer from Plant A

[[

]]

Figure 12: Peak hold RMS frequency spectra for pressure transducer at Plant A.

[[

]]

Figure 13: Peak Hold RMS frequency spectra from pressure transducer at Plant C.

[[

]]

Figure 14: Trend of RMS pressure amplitude vs. steam flow at Plant A.

[[

]]

Figure 15: Frequency spectra from pressure transducer on inside and outside steam dryer skirt at Plant A.

[[

]]

Figure 16: 0-Peak power ascension colormap from strain gauge on vertical hood at Plant A.

[[

]]

Figure 17: Peak Hold RMS frequency spectra from strain gauge mounted on inner hood at Plant C.

[[

]]

Figure 18: Peak Hold RMS frequency spectra from strain gauge mounted on outer hood at Plant A.

[[

]]

Figure 19: Representative peak hold frequency spectrum at 100% power for Plant A.

[[

]]

Figure 20: Representative peak hold frequency spectrum at 100% power for Plant B.

[[

]]

Figure 21: Representative peak hold frequency spectrum at 100% power for Plant C.

[[

]]

Figure 22: Velocity streamlines adjacent to the outer hood and MS nozzles in a QC1 style steam dryer

[[

]]

Figure 23: Velocity streamlines adjacent to the outer hood and MS nozzles in a QC1 style steam dryer

[[

]]

Figure 24: In vessel visual examination data of steam dryer outer hood.

4.0 Scale Model Test Methods and Apparatus

The physical mechanisms responsible for the excitation of flow-acoustic resonances are not easily modeled using purely analytic methods. Recognizing that it is often prohibitively expensive to instrument an operating reactor for operational testing and considering the impossibility of making parametric changes to the plant configuration it was decided to pursue model testing of the Quad Cities plant configurations to investigate the possible existence of acoustic loads in the steam system. Oftentimes model tests prove to be an effective and efficient method for investigating Flow Induced Vibration (FIV) problems in power plant systems. It is usually not practical to build a full scale model of the system of interest; therefore, small scale models are typically used as an alternative. Prior to designing a model, the important phenomena must be identified so that they may be preserved in the model. Similitude is used to preserve important dimensionless parameters between the full scale system and the model system to enable successful model testing.

4.1 Scale Model Relationships

Several phenomena have been suggested which could impose oscillating pressure loadings on the steam dryer. These include acoustic pressure oscillations induced by flow turbulence and vortex shedding from various parts of the structure.

It was recognized early on that both the Mach Number and Reynolds number could not be preserved in the same model. To do so using ambient air as the desired test fluid would require a model substantially larger than the actual plant. Considering that the available plant data provided strong support for acoustic induced vibration of the steam dryer and that the plant Mach number is low it was apparent that the system natural frequencies could be predicted in the model by ensuring geometric similarity between plant and model. Also noting that the plant data strongly suggested that the BWR vessel steam plenum is susceptible to aero-acoustic resonances of the safety and relief valve standpipes excited by shear layer instabilities or vortex shedding it was decided to preserve the Mach number rather than the Reynolds number in the model. The decision

to preserve Mach number rather than Reynolds number to investigate the possibility of an aero-acoustic resonance in the safety and relief valve standpipes is supported by the observation that the vortex shedding frequency for many configurations is relatively independent of the Reynolds number [2]. This observation alone is not sufficient to dismiss the possible importance of Re; however, it was decided that the Re was of secondary importance.

One way of demonstrating the importance of maintaining geometric similarity and preserving the Mach number is to examine the ratio of the vortex shedding frequency to the acoustic frequency. Recalling the assumption that St is independent of Re:

$$\frac{Vortex\_Shedding}{Acoustics} = \frac{\frac{St \cdot U}{d}}{\frac{c}{L}} \approx St \cdot \frac{U}{c} \cdot \frac{L}{d}$$

The expression above simplified to the product of the St, which is assumed to be constant, the Mach Number and the geometric scaling factor.

Moody [12] non-dimensionalized the continuity equation and conservation of momentum equation and estimated the relative importance of various non-dimensional groups. From this work he showed that the Mach number, typically associated with acoustical phenomena, was the most significant parameter. The Reynolds number did not appear to be a significant parameter for the phenomena being studied.

Studies have been performed to both strengthen and justify the assumption regarding Reynolds number. Malone [13] performed unsteady CFD analyses on a simplified BWR model at Reynolds numbers that spanned the plant and the model facility. These evaluations showed that the same flow patterns were observed in both scales. This observation suggests that the important phenomena are preserved in the scale model; therefore, the model is a useful tool to investigate the BWR behavior. Figure 22 is an

excerpt from Reference [13] which shows the fluid velocity streamlines in the steam plenum adjacent to the outer hood.

References 11 and 12 provide a detailed discussion of the scaling laws applied to the scale model test apparatus. Reference 14 describes a successful scale test program which used a similar frequency scaling approach to investigate shear layer instability induced acoustic resonances. Assuming that the Strouhal number is not a strong function of Reynolds number, and if the Mach number in the plant is preserved in the model, and ensuring geometric similarity between both systems, both the vortex shedding and acoustic frequencies are related by the length and velocity ratios. Frequency and pressure measurements in the scale model can be used to predict frequencies and pressures in the full size system. The frequency and pressure scaling relationships are summarized below:

[[

]]

4.2 Test Apparatus

Figure 25 is a schematic of the model BWR acoustic test apparatus designed for this test program. The BWR model extends from the steam/water interface inside the Reactor Pressure Vessel (RPV) out the steam lines to the turbine inlet. Ambient air is used as the test fluid. The test apparatus is composed of two primary components:

1. Test fixture
2. BWR model

The test fixture consists of the components necessary to provide the required air flow to the model. The model consists of the steam dryer, RPV, and steam lines. Both the test fixture and the model are described separately below.

The test fixture consists of the following components:

[[

]] which is routed through the inlet piping into the model. A venturi flow meter and muffler have been mounted between the blowers and the scale model. The venturi flow meter is used to measure the total system air flow and the muffler is used to isolate the model from the noise introduced into the system by the test fixture. This noise may consist of the blower Vane Passing Frequency (VPF), organ pipe modes associated with the inlet piping, or other broadband noise created by the test fixture configuration.

The BWR model consists of three components:

[[

]]

The model scale is determined by the flange diameter to which the BWR mockup is attached; therefore, plants with different RPV diameters would be modeled at different scales. The QC model is built to a 1:17.3 scale. [[

]] Figures 26 through 32 are images of the test apparatus and BWR models designed for these tests.

Most dimensions used to build the model were taken from GE design drawings. Where possible, as-built dimensions of the main steam lines provided by Exelon Generating Company, LLC were used for the MSL model. [[

]]

4.3 Modeling Assumptions

It is recognized that no model is an exact replica of the system under investigation; simplifying assumptions must always be made. This section presents the assumptions and simplifications used to build the BWR scale model used in the tests, and provides the justification that these simplifications and assumptions are adequate

4.3.1 BWR Components Omitted

The following components are not present in the scale model of the steam system:

[[

]]

4.3.2 BWR Components Approximated

The following components are included; however, specific assumptions have been made which affect the manner in which they are modeled in the system.

[[

:

]]

4.3.4 Environmental differences

The following differences exist between the environmental parameters at the test scale and the full scale:

[[

]]

4.3.5 System Configuration

The following differences exist between the system configuration used for the test program and the full scale system configuration:

[[

]]

4.4 Data Acquisition System

Acoustic pressures were measured using electret microphones located in both the MSL and the RPV. Total system flow was measured using a calibrated venturi and Rosemount pressure transducer. For some tests the air flows in the individual MSLs were measured using a velocity probe in each line. Air temperatures in the system were measured using K-type thermocouples in the RPV on the steam dryer cover plate and at the turbine inlet in the MSL.

The analog time history data was sampled using a LMS SCADAS III dynamic signal analyzer. The SCADAS III performs the analog to digital conversion necessary so that the sampled data can be stored as a throughput file on the test computer. A Dell D600 Latitude with 1 Gigabyte of RAM running the LMS Test.Lab 5A SL1 software was used for the data acquisition and analysis.

4.5 Sensor Locations

Tests were performed with both the original and replacement QC steam dryer models installed in the test apparatus. Microphones were installed in the main steam lines as well as on the dryer surfaces. All microphones were mounted such that the sensor diaphragm was placed flush with the steam dryer outer surfaces or the MSL inner surface. Forty-one (41) microphone locations were defined on the main steam lines; however, not all locations were used for each test. Figure 33 identifies the microphone locations specified in the main steam lines. The following main steam line locations were instrumented:

[[

]]

Fifty-two (52) locations were defined on the original QC dryer and fifty-six (56) locations were defined on the replacement steam dryer. Figures 34 and 35 identify the microphone locations chosen for each dryer. The locations were chosen to be consistent with observed failures on the original dryer, the in-vessel instrumentation to be installed on the replacement dryer, and to obtain an understanding of the spatial pressure distribution around the dryer. Not all locations were used for each test. The following regions were instrumented on each dryer:

[[

]]

[[

]]

Figure 25: General schematic of GE scaled test apparatus

[[

]]

Figure 26: Test apparatus

[[

]]

Figure 27: Steam dryer models, original (Left) & replacement (Right)

[[

]]

Figure 28: Close Up view of scale model identifying major components

[[

]]

Figure 29: Main Steam Isolation Valves

[[

]]

Figure 30: D-Ring Equalizing Header

[[

]]

Figure 31: Turbine Stop and Control Valves

[[

]]

Figure 32: Turbine Inlet

[[

]]

Figure 33: Scale model main steam line sensor locations.

[[

]]

Figure 34a: Original dryer sensor locations

[[

]]

Figure 34b: Original dryer sensor locations

[[

]]

Figure 34c: Original dryer sensor locations

[[

]]

Figure 34d: Original dryer sensor locations

[[

]]

Figure 34e: Original dryer sensor locations

[[

]]

Figure 35a: Replacement dryer sensor locations

[[

]]

Figure 35b: Replacement dryer sensor locations

[[

]]

Figure 35c: Replacement dryer sensor locations

[[

]]

Figure 35d: Replacement dryer sensor locations

[[

]]

Figure 35e: Replacement dryer sensor locations

[[

]]

Figure 35f: Replacement dryer sensor locations

5.0 Data Analysis Methods

This section provides a description of the data acquisition, reduction and analysis performed for the Quad Cities 1 tests.

5.1 Data Acquisition

Section 4 provides details of the sensor locations and types used for the testing. A LMS SCADAS III data acquisition front end controlled by a PC equipped with LMS Test.Lab software, revision 5A SL1, received the transducer signals as analog voltages. The specific software module used during data acquisition was Signature Testing with the Time Recording During Signature Acquisition add-in. The front end performs an analog to digital conversion on the signal and transfers the signal to the PC where all of the signals from one run are stored in a throughput file, which is a LMS format of amplitude versus time. The initial digitization was performed with the following parameters:

- 16384 Hz sampling rate
- AC coupling on dryer pressure transducer signals
- DC coupling on venturi and vessel pressure transducer signals and thermocouple signals
- Approximately 60 seconds of raw time data (throughput) recorded for dwells
- Approximately 500 to 600 seconds of raw time data (throughput) recorded for the 130 cfm to 225 cfm sweep (the whole sweep was captured – the time recording was stopped once the sweep had reached its upper flow limit)

All test equipment were calibrated prior to initiating the testing described in this document. In addition, an "end-to-end" calibration check was performed for each microphone before and immediately after all tests. This step ensured that the instrumentation remained functional and exhibited sensitivities consistent with their calibration values. This also ensured that any instrumentation that may have

malfunctioned during a test evolution were identified after the test so that the data could be treated accordingly.

5.2 Data Processing

The data processing involved the conversion of the raw time data for the dryer pressure sensors and the main steam line pressure sensors in the throughput files (or original raw time domain data files) to the following output formats:

- Peak Hold Autopower Spectra
- Peak Hold Autopower Spectra with amplitude and frequency scaled from subscale to full scale
- Linear Averaged Autopower Spectra
- Phase Referenced Frequency Spectra/Operating Deflection Shape
- RMS Level of Frequency Band versus time and flow

The LMS software module used for processing was Throughput Validation and Processing Host with the following add-ins:

- Signature Throughput Processing
- Time Signal Calculator
- Geometry
- Operating Deflection Shape
- Signature Post-Processing

5.2.1 Peak Hold Autopower Spectra

The peak hold autopower spectra were processed from the throughput files with the following parameters:

- 0 Hz to 6400 Hz frequency range
- 1 Hz frequency resolution
- Hanning Window
- 0 to peak amplitude
- linear (square root of autopower) units
- linear or no weighting
- peak hold averaging
- 2 averages per second

5.2.2 Peak Hold Autopower Spectra Scaled to Full Scale

The peak hold autopower spectra as processed above were exported to Excel. In Excel, the frequency resolution was reduced by the frequency scaling factor and the spectral amplitude was increased by the pressure scaling factor to correct the model data to plant conditions. These scaling factors were calculated using the scaling relationships shown in equations (10) and (11) described in Section 4.1. The pressure scaling factor determined using equation (11) was conservatively increased by approximately 25% :

[[

]]

5.2.3 Linear Averaged Autopower Spectra

Linear averaged autopower spectra were processed from the dwell throughput files using the following parameters:

- 0 Hz to 6400 Hz frequency range
- 1 Hz frequency resolution
- Hanning Window
- 0 to peak amplitude
- power units for the dwell condition, linear (square root of autopower) units for the sweep
- linear or no weighting
- linear averaging
- 2 averages per second for the dwell condition
- 1 spectrum every 5 seconds for the sweep condition

5.2.4 Linear Averaged Crosspower Spectra

Linear averaged crosspower spectra were processed from the throughput files using the following parameters:

- 0 Hz to 6400 Hz frequency range
- 1 Hz frequency resolution
- Hanning Window
- 0 to peak amplitude
- power units
- linear or no weighting
- linear averaging
- 2 averages per second for the dwell condition
- Original Dryer Reference Sensor: M26 dynamic pressure

- Replacement Dryer Reference Sensor: M136 dynamic pressure

The linear averaged crosspower spectra were used to produce operating deflection shapes from the dwell condition.

5.2.5 Phase-referenced Frequency Spectra

Phase-referenced frequency spectra were processed from the throughput files using the following parameters:

- 0 Hz to 6400 Hz frequency range
- 1 Hz frequency resolution
- Hanning Window
- 0 to peak amplitude
- power units
- linear or no weighting
- linear averaging
- 1 measurement every 5 seconds for the sweep, and 1 measurement every 1 second for the dwell
- Original Dryer Reference Sensor: M26 dynamic pressure for the post-processed data, M25 dynamic pressure for the online-processed data
- Replacement Dryer Reference Sensor: M136 dynamic pressure

The result of phase referencing is that the frequency spectrum of the reference has 0° phase throughout the frequency range, and the phase of the other transducers is adjusted so that for each frequency line the phase is with respect to the reference instead of the start of the measurement time record. The phase-referenced frequency spectra from the sweep using M26 as the reference were used to produce operating deflection shapes from the sweep condition. The phase referenced-frequency spectra using M25 as the reference were only used for examining system trends

5.2.6 RMS Level of Frequency Band versus time and flow

For the sweep, frequency bands were selected by visually reviewing the waterfall and using cursors to select borders of frequency bands that appeared significant. The rms level of these bands was calculated and was plotted versus time and flow rate.

6.0 Scale Model Test Results

This section describes the tests performed and summarizes the critical results and conclusions. Considering the number of sensor locations defined and the substantial number of tests performed, this document cannot present all data acquired from all tests. The data presented herein are considered to be representative of the general system behavior.

6.1 Test Purpose

The goals of the QC steam dryer tests were to:

1. Establish an understanding of the baseline behavior of system

2. Obtain fluctuating pressure time history data that can be used to develop a dryer load definition

3. Identify possible sources of the fluctuating pressures observed in the system

4. Develop an explanation of the observed frequency content

The tests described here are the first model tests performed on a complete model of a BWR steam system; therefore, these data constitute a first look into the acoustic behavior of the steam system. These tests are the first steps toward developing a more thorough understanding of the expected dryer loads. As such they are the beginning of an extensive amount of ongoing research into both the excitation mechanisms and critical component geometries as well as development of a robust load definition methodology.

6.2 Summary of Testing Performed

To satisfy the goals described above, three distinct test evolutions were performed:

- Baseline Testing
  - Original Dryer Configuration
  - Replacement Dryer Configuration
- Source Screening Tests
  - Original Dryer Configuration
  - Replacement Dryer Configuration
- Characterization Testing
  - Replacement Dryer Configuration

All frequencies reported in this section are model frequencies. The equivalent plant frequency can be determined by applying the frequency scaling factor listed in Section 5.2.2.

6.2.1 Baseline Tests

These tests were performed to acquire data throughout the range of expected plant operating conditions from which a general understanding of the system behavior could be obtained. These data were also used to benchmark the model against in-plant data. Sweep and dwell tests were performed with both dryer configurations. The model flow rates calculated for OLTP and EPU power conditions at the plant were determined using the requirement that [[ ]]. The model flow rates which correspond to specific power levels in the full scale can be determined as follows:

[[

]]

Model testing has confirmed that the flow rate in each MSL is approximately ¼ of the total flow rate; therefore, the total model flow rates measured at the venturi for OLTP and EPU conditions are:

[[

]]

The test fluid static pressure and temperature remained within the following range for all tests:

[[

]]

6.2.2 Source Screening Tests

Source screening tests were performed to identify which components controlled the observed frequency content of the fluctuating pressures in the steam plenum. The following components were investigated:

[[

]]

Each of the components identified above is shown in Figure 36.

[[

]]

The contribution from a specific component was identified by comparing the response in the steam plenum measured for each test configuration.

6.2.3 Characterization Tests

Characterization testing was performed to acquire data that could be used to correlate the acoustic Finite Element Model (FEM) of the test apparatus. The acoustic FEM was used to predict the normal modes of the steam system; these modes were then used to help interpret the frequency content and spatial pressure distribution of the data acquired in the steam plenum. The acoustic FEM is discussed in more detail in Section 6.3.4.2.

The characterization testing was performed by injecting a known noise source at various locations in the physical model and measuring the response at other locations. Frequency Response Functions (FRF) calculated from the test data were compared against FRFs calculated from the acoustic FEM to identify deficiencies in the acoustic FEM. The acoustic FEM was then modified, where appropriate, to improve the correlation. These tests were performed both with and without flow in the system. The RPV and MSL models were first correlated separately and then a final correlation was performed with both the RPV and MSL combined.

6.3 Summary of Model Data

The scale model data acquired from the tests described above are summarized in the following order:

- Baseline Test Data Characteristics
- Comparison of Original Dryer and Replacement Dryer test data
- Discussion of Source Screening Test Data

- Preliminary Source Identification and Explanation of Steam Plenum Frequency Content

The data presented in this section are reported in the model scale. These data must be corrected to the plant scale using the frequency and pressure scaling factors described in Section 5.2.2 to compare them with the plant data presented in Section 3.

6.3.1 Baseline Test Data Characteristics

This section provides data that describe the general trends observed in the original and replacement dryer tests.

6.3.1.1 System Trends versus Flow

Figure 39 is a color map exhibiting the trend of fluctuating pressure amplitude with model flow rate. The horizontal axis displays frequency, the vertical axis corresponds to reactor power level and the color scale depicts fluctuating pressure amplitude. [[

]]

It is also evident that there are multiple frequencies observable in the data. To better understand the trend of fluctuating pressure amplitude with flow rate at each frequency, the RMS pressure amplitudes for frequency bands centered around some of the frequencies observable in Figure 39 are displayed in Figure 40. The trends shown in Figure 40 have also been fit with power law equations so that they can be compared to

the plant data presented in Section 3.2.2. Although the trends shown in Figure 40 are from the outer hood of the replacement dryer they are representative of the data obtained from both dryer designs and from multiple sensors located around the dryer. It is apparent that the pressure oscillations can be approximated by the following relationship:

$$P = A \cdot U^b \qquad (1)$$

Where: P is the fluctuating pressure amplitude
A is a reference pressure
U is the mean fluid velocity
b is the power law exponent,
[[

]]

6.3.1.2 Spatial Distribution of Fluctuating Pressures

Figures 41 and 42 exhibit the general vertical distribution of fluctuating pressures in the dryer region close to the MSL nozzles for both the original and replacement dryer designs. [[

]]

This behavior is consistent with the normal modes predicted using the acoustic FEM and will be discussed in more detail in Section 6.3.4.2.

6.3.1.3 OLTP & EPU Frequency Spectra

[[

]]

6.3.1.4 System Repeatability

To assess system repeatability multiple tests were repeated throughout a day and on separate days. Figures 43 and 44 are frequency spectra of the model data obtained during the repeatability tests. Figure 43 displays data obtained from the outer hood (Original Dryer Microphone 14) at different times during the same day. Between each run reported in Figure 43 the test apparatus configuration had been changed to perform other tests and then returned to the repeatability test configuration. Figure 44 presents data obtained from a sensor placed on the steam dryer skirt (Original Dryer Microphone 26) for runs performed at different times during the same day and on different days. The figure legends identify the sensor group (ga or gb) as well as the repeated run on each day (r2, r3). Group A and Group B tests were performed on different days. Observation of Figures 43 and 44 shows that the system exhibits the same frequency content and amplitude for test runs made with the same configuration both on the same day and on different days. The data obtained from six tests performed on two separate days using the same configuration demonstrate that the scale test facility and the QC1 scale model produce consistent and repeatable results.

6.3.1.5 Model Data used for Load Definition

[[

]]

6.3.2 Comparison of Original and Replacement Dryer Data

Frequency spectra from comparable sensor locations were overlaid on the same axes to assess the difference in the fluctuating pressure loads predicted for the two dryer designs. Figures 45 through 47 show comparisons of the measured spectra from the top plates, outer hood, and skirt. RMS pressures in the following three frequency bands were also calculated: 5-3200 Hz, 5-1200 Hz, 1200-3200 Hz. Figures 48 through 50 display the RMS pressures calculated for each of these frequency bands.

[[

]]

6.3.3 Discussion of Source Screening Test Data

The apparent effect of each component on the steam plenum fluctuating pressure loads was determined by a comparison of the frequency spectra obtained from the tests performed with and without the specific component. If a change in the frequency content or amplitude was observed in the steam plenum when the component was absent then the component was considered to be a possible source or important resonator. Using this simple criterion the following components were shown to have a strong effect on the dryer loads:

[[

]]

The remaining components discussed in Section 6.2.2 were not observed to have a significant affect on the dryer loads.

6.3.3.1 MSL Source Screening Test Observations

[[

]]. Recognizing this, the amount of the observed effect contributed by individual components contained in the removed section is not immediately obvious. This limitation is not problematic because this test was only intended to obtain an initial assessment of the relative importance of the various components.

Figures 51 through 53 summarize the data discussed in this section. Figure 51 represents data acquired from Replacement Dryer sensor 136 which is located on the skirt. [[

]] The top half of each figure displays a linear average spectrum; whereas, the bottom half of the plot is a peak hold spectrum. The nomenclature used in the figure header to refer to the test performed at each cut line is explained in Table 7 below:

Table 7: Identification of MSL Source Screening Test header nomenclature

[[

]]

Figure 55 summarizes the percent of the baseline RMS pressures measured for each test condition. This figure provides a quantitative estimate of the signal content remaining in the steam plenum for each test. The five frequency bands shown in Figure 55 are slightly different than shown in Figures 51 through 54 and were chosen to highlight the significant frequency content observable in the steam plenum: [[

]]

[[

]]

6.3.3.2 MSIV Source Screening Test Observations

[[

]]

Table 8 shows the percent change in the RMS fluctuating pressures calculated from the spectra shown in Figures 56 through 58. A negative number represents a load reduction; whereas, a positive number represents an increased load. Frequency bands containing the most significant frequency content were chosen.

[[

]]

6.3.3.4 Remaining MSL Components Considered in Source Screening Tests

[[

]].

6.3.4 Source Identification and Explanation of Frequency Content

The testing performed to date has shown that the frequency content observed in the model steam plenum can be segregated into three separate groups for discussion of source mechanisms and critical resonating chambers:

[[

]]

An acoustic finite element model of the test apparatus was built to assist in the interpretation of the scale model test data. The LMS VL.Acoustics and Sysnoise Finite Element Analysis software was used for this analysis. Figures 61 and 62 show the finite element mesh used to model the steam plenum and main steam lines. [[

]]

The model was correlated to the test apparatus using the test data acquired during the characterization tests described above. Figure 63 shows an overlay of some of the experimental and analytical FRFs which indicate a generally good correlation between the model and the test apparatus. Characterization tests were also performed at various flow rates to show that the acoustic FEM could adequately replicate the system normal modes at the flow rates of interest. It is recognized that the Mach number in the system is low; therefore, it was assumed that the normal modes would not be largely affected by the mean flow. To be thorough, some of the correlation testing was performed with flow in order to confirm this assumption.

Once the model was correlated then the normal modes predicted by an acoustic modal analysis were used to help interpret the data measured in the steam plenum. Figures 65 through 69 show the first nine steam plenum acoustic cavity modes for the test apparatus. These modes can be scaled to plant conditions using the same frequency scaling factor discussed above. It can be observed that these modes all exhibit the highest modal

pressures in the dryer skirt region which is consistent with the trends observed in the model data.

6.3.4.2.2 Test Data Characteristics in Steam Plenum

[[

]]

6.3.4.4 Summary of Frequency Content

The discussion of the observed frequency content and postulated excitation mechanisms discussed above are summarized:

[[

]]

6.4 Applicability of QC1 Model Data to QC2

Although the scale model was built to represent Quad Cities Unit 1, the instrumented steam dryer will be installed in Quad Cities Unit 2. The QC 1&2 steam system configurations are compared to assess whether the Quad Cities Unit 1 model data is applicable to Quad Cities Unit 2. Both Quad Cities vessels were built to the same set of design drawings; therefore, the RPV dimensions are the same (within the fabrication tolerance). In addition, the same replacement dryer design is used for both units. The total MSL lengths for the two units are effectively the same; however, there are some minor differences between the steam lines at each unit. The HPCI branch line is attached to MSL B at QC1 and MSL D at QC2. The location and type of safety and relief valves are different between both Quad Cities units; however, the difference in location with respect to the vessel is not substantial. There are also expected to be some minor differences in lengths between elbows, valves, etc. between each unit.

Considering the explanation of the frequency content provided in Section 6.3 and the comparison of the two units provided above it is expected that the lower frequency content considered to be associated with the MSL organ pipe modes will not vary significantly between the two units. In addition, the RPV acoustic modes will be identical for the two units. Although the exact location of the safety and relief valves are slightly different between the two units, the standpipe lengths, steam flow rates and branch line diameters are the same. The frequencies associated with the SV should be equivalent as well.

Considering that the plant layouts are almost identical, each of the sources present in Quad Cities Unit 1 should also be present in Quad Cities Unit 2; therefore, the amplitude of the response measured in QC1 is considered representative of the expected response in QC2.

The Quad Cities Unit 1 model data is considered applicable to both Quad Cities Unit 1 and Quad Cities Unit 2.

6.5 Preliminary Justification of Model Pressures and Frequencies

As mentioned above, there is no existing in-vessel Quad Cities plant data that can be used as a benchmark for the scale model data. The in-vessel data necessary to benchmark the model data is currently expected to be available during the Summer of 2005. In the interim, it is important to gauge, as well as possible, the validity of the scale model and scaling relationships. Section 3 describes the available in-vessel data. Although none of the three plants from which data is available is an exact replica of the QC plant configuration this data does provide a very good benchmark. The benchmark is performed in three steps:

1. Compare fluctuating pressure trends
2. Compare general frequency content
3. Compare fluctuating pressure amplitudes at equivalent flow rates

It should be recognized that Plant A has different steam lines and a smaller vessel than QC1; however, both plants have square hood dryers. Recalling the similarity between the fluctuating loads observed in Plants A, B, and C in Section 3, the same phenomena should be present in both Plant A and Quad Cities Units 1 & 2. Considering this, the data from Plant A and QC should possess distinct similarities regarding frequency content and trends. This is not surprising considering that the overall geometries and operating regimes for GE BWRs are similar.

First, the general trends observed in both the plant and model data are discussed. [[

]] It can be concluded that the model and plant data each appear to behave similarly.

Next, the frequency content between the model data and the plant data are compared. [[

]]

Figures 73 and 74 compare a peak hold frequency spectrum obtained from model QC1 original dryer data to a peak hold frequency spectrum obtained from Plant A data at comparable locations on the dryer skirts. Figure 73 displays amplitudes determined using the pressure scaling relationship including the conservative factor of 1.25. Figure 74 displays amplitudes using the true pressure scaling factor calculated using the pressure scaling relationship without the additional factor of 1.25. [[

]]

In Section 3 it was shown that each of the three plant data sets available exhibited very similar general data trends as well as frequency and amplitudes; therefore, it is expected that the QC1 model would also correlate well with Plants B and C.

The critical observations that should be made from this comparison are:

1. The same phenomena occur in both the plant and the model data

2. The frequency bands are consistent

3. The trend of fluctuating pressures are consistent

4. The difference in the frequencies observed at each plant for each band is consistent with the difference between the physical dimensions of the plants

5. The frequencies predicted using the scale model show very good agreement with the available plant data.

6. The amplitudes of the fluctuating loads in the scale model appear to be conservative with respect to the available plant data.

Using the information available today it can be said that the GE scale model test apparatus and scaling methodology produce a plant data prediction that matches the available plant data very well. The model appears to provide a conservative estimate of the expected plant loads acting on the steam dryer.

The scale model data will be benchmarked against the Quad Cites in-vessel data when they are available.

[[

]]

Figure 36: MSL Components considered in the source screening tests.

[[

]]

Figure 37: Locations at which the MSL was removed for the MSL source screening test.

[[

]]

Figure 38: Schematic of typical BWR Main Steam Isolation Valve

[[

]]

Figure 39: Colormap of Replacement Dryer test data, Microphone 125, 80-135% power.

[[

]]

Figure 40: Trend of model fluctuating pressures with mean MSL velocity for selected outer hood data.

[[

]]

Figure 41: Vertical spatial pressure distribution, Replacement Dryer, EPU power.

[[

]]

Figure 42: Vertical spatial pressure distribution, Original Dryer, EPU power.

[[

]]

Figure 43: Original Dryer Sensor 14 Repeatability test data

[[

]]

Figure 44: Original Dryer Sensor 26 Repeatability test data

[[

]]

Figure 45: Comparison of Original and Replacement Dryer loads, Top Plates.

[[

]]

Figure 46: Comparison of Original and Replacement Dryer loads, Outer Hoods.

[[

]]

Figure 47: Comparison of Original and Replacement Dryer loads, Skirt.

[[

]]

Figure 48: Comparison of RMS pressures for original and replacement dryer designs, 5-3200 Hz.

[[

]]

Figure 49: Comparison of RMS pressures for original and replacement dryer designs, 5-1200 Hz.

[[

]]

Figure 50: Comparison of RMS pressures for original and replacement dryer designs, 1200-3200 Hz.a

[[

]]

Figure 51: Frequency spectra for MSL source screening tests, 5-2500 Hz.

[[

]]

Figure 52: Frequency spectra for MSL source screening tests, 5-300 Hz.

[[

]]

Figure 53: Frequency spectra for MSL source screening tests, 20-1200 Hz.

[[

]]

Figure 54: Frequency spectra for MSL source screening tests, 1500-1800 Hz.

[[

]]

Figure 55: Percent of baseline RMS pressure measured in steam plenum for MSL source screening test.

[[

]]

[[

]]

[[

]]

[[

]]

[[

]]

Figure 60: Identification of separate frequency bands in model data..

[[

]]

Figure 61: Acoustic FEM cavity mesh and skin mesh of QC1 steam plenum and dryer surfaces

[[

]]

Figure 62: Acoustic FEM mesh of the entire QC1 model steam system.

[[

]]

Figure 63: Subset of Acoustic FEM correlation results to characterization test data.

[[

]]

[[

]]

[[

]]

[[

]]

[[

]]

[[

]]

[[

]]

Figure 73: Comparison of QC1 model data with Plant A in-vessel data using pressure scaling factor used for load definition.

[[

]]

Figure 74: Comparison of QC1 model data with Plant A in-vessel data using true pressure scaling factor without conservative factor of 1.25

7.0 Summary and Conclusions

The following conclusions are made from the information presented above:

1. Using the available plant data, acoustic induced vibration is considered to be the most significant load on the steam dryer.

2. The scale model test data matches well with the available in-plant data; therefore,

    a. The scale model test apparatus and methodology are viable tools to predict fluctuating pressure loads on the steam dryer.

    b. The decision that acoustic loads are the primary contribution to the fluctuating loads on the BWR steam dryer is validated.

    c. The model data appear to be conservative in the 30-100 Hz frequency band at the plant scale.

    d. Considering the startup testing and acceptance criteria planned for the QC replacement dryer, the QC model data acquired from the Baseline tests is considered an acceptable input for a QC dryer load definition.

2. The sources for the fluctuating pressures acting on the dryer can be explained by the following:

    [[

4. Recognizing the similarity between the QC1 & 2 steam plenum and steam line designs, the QC1 model data is considered to be applicable to both Quad Cities Unit 1 & 2.

The scale model data will be benchmarked against the Quad Cites in-vessel data when they are available. Additional work is on-going to improve the understanding of the excitation mechanisms and source locations. The work described in this document is the beginning of a substantial amount of research focused on developing predictive tools that can be used to define accurate load definitions for BWR steam dryers.

8.0 References

1. Au-Yang, M. K., "Flow-Induced Vibration of Power and Process Plant Components", Professional Engineering Publishing Limited, 2001.

2. Blevins, R. D., "Flow Induced Vibration", 2nd Edition. Krieger Publishing Company. 2001.

3. Ziada, S., Buhlmann, E.T., Bolleter, U., "Flow Impingement as an Excitation Source in Control Valves", Journal of Fluids and Structures, 3, 529-549.

4. Graf, H.R., Ziada, S., Rohner, R., Kalin, R., "Verification of Scaling Rules for Control Valve Noise by Means of Model Tests", AD-Vol. 53-2, Fluid-Structure Interaction, Aero elasticity, Flow-Induced Vibration and Noise, Volume II, ASME 1997.

5. Ziada, S., Sperling, H., Fisker, H., "Flow-Induced Vibration of a Spherical Elbow Conveying Steam at High Pressure", PVP-Vol 389, Flow-Induced Vibration. 1989.

6. Ziada, S., "A Flow Visualization Study of the Flow-Acoustic Coupling at the Mouth of a Resonant Side-Branch". ASME Pressure Vessel and Piping Journal. Vol 258. pp. 35-59. 1993.

7. Baldwin, R. M., Simmons, H. R., "Flow-Induced Vibration in Safety Relief Valves", Journal of Pressure Vessel Technology, Vol. 108, Aug. 1986, pp. 267-272.

8. Rockwell, D., Naudascher, E., "Review – Self-Sustaining Oscillations of Flow Past Cavities", Journal of Fluids Engineering, Vol. 100, June 1978, pp. 152-165.

9. Elmore, W.C., Heald, M. A., "Physics of Waves". Dover Publications. 1969.

10. Ziada, S., "A Flow Visualization Study of the Flow-Acoustic Coupling at the Mouth of a Resonant Side-Branch". ASME Pressure Vessel and Piping Journal. Vol 258. pp. 35-59. 1993.

11. Lynch, J., "Scaling of the Miniature Steam Dome, Revision 1". December 2, 2002.

12. Moody, F.J., "Root Cause Scale-Modeling Rationale for the Quad Cities Dryer Incident". September 9, 2002.

13. Malone, Bobby. "Computational Fluid Dynamics Flow Visualization of Quad Cities Sub-Scale Original Dryer Model as a Function of Reynolds Number". NEDC-33191P. April 2005.

14. Ziada, S., Buhlmann, E. T., Bolleter, U. "Flow Impingement as an Excitation Source in Control Valves".

15. Morse, Philip M., Ingard, K. Uno., "Theoretical Acoustics". Princeton University Press. 1986.